Electronic structure of polyacetylene: Optical and infrared studies of undoped semiconducting (CH)$_x$ and heavily doped metallic (CH)$_x$

C. R. Fincher, Jr., M. Ozaki,* M. Tanaka,† D. Peebles, L. Lauchlan, and A. J. Heeger

Department of Physics and Laboratory for Research on the Structure of Matter, University of Pennsylvania, Philadelphia, Pennsylvania 19104

A. G. MacDiarmid

Department of Chemistry and Laboratory for Research on the Structure of Matter, University of Pennsylvania, Philadelphia, Pennsylvania 19104

(Received 23 January 1979)

The band structure and electronic properties of pure and heavily doped polyacetylene (both as grown and stretch oriented) have been investigated by a combination of optical-absorption and -reflection measurements in the frequency range from the middle ir (0.1 eV) through the visible (4.0 eV). The absorption data are consistent with a direct gap of approximately 1.4 eV in the trans-(CH)$_x$. A Kramers-Kronig analysis of the reflection data has been carried out to obtain $\sigma(\omega)$ and $\epsilon(\omega)$. We find that for the undoped semiconducting polymer, the strong transition observed in the visible exhausts the oscillator strength sum rule for π electrons consistent with an interband transition. The frequency-dependent conductivity obtained from Kramers-Kronig analysis of the metallic polymer reflection data suggests "interrupted-strand" behavior. Application of effective-medium theory implies an intrinsic dc conductivity for metallic [CH(AsF$_5$)$_{0.15}$]$_x$ of $\sigma > 2 \times 10^4$ Ω^{-1} cm^{-1}. The measured dc values have thus far been limited by the low-density fibril morphology.

I. INTRODUCTION

The electronic structure of polyenes has been a subject of interest for many years. The unsaturated bonds which characterize the polyenes have an important effect on their electronic structure and the corresponding electronic properties. In a polyene (see Fig. 1, for example) three of the four carbon valence electrons are in sp^2 hybridized orbitals; two of the σ-type bonds are links in the backbone chain while the third forms a bond with some side group (e.g., H in Fig. 1). The remaining valence electron has the symmetry of the $2p_z$ orbital and forms a π bond in which the charge density is perpendicular to the plane of the molecule. In terms of an energy-band description, the σ bonds form low-lying completely filled bands, while the π bond would correspond to a half-filled band. The π bond could be metallic provided there is negligible distortion of the chain, and an independent-particle model proved to be satisfactory.

The possibility of a distortion of the molecular structure intrigued the early investigators. Lennard-Jones,[1] in an early application of Hückel theory of molecular orbitals, investigated the electronic structure of polyenes. His conclusion, that in the limit of an infinite chain the bonds tended to a constant value of 1.38 Å, was later supported by studies of Coulson.[2] However, the theoretical conclusions seemed less than satisfactory in view of the experimental observations.[3] Using either molecular-orbital (MO) theory or a free-electron model in which the π electrons are considered free to delocalize along the chain, the energy for a

transition to the lowest excited state decreases linearly with the reciprocal of the chain length. This rule was observed to work rather well for the short polyenes. However, experiments indicated that for very long chains the transition energy reached a limiting value of about 2 eV.[3] Later Kuhn[4] demonstrated that bond alternation could
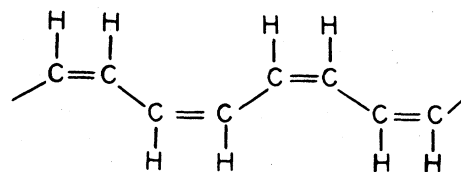
CIS
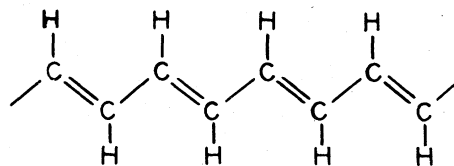
TRANS

FIG. 1. Molecular structure of *cis* and *trans* isomers of polyacetylene, (CH)$_x$.

serve as a possible explanation of the energy gap in long polyenes.

The first convincing analysis was that given by Lounget-Higgins and Salem[5]; by assuming a well-defined model they were able to carry out the calculation without recourse to estimates of physical parameters. Considering this simple model, we begin with a chain consisting of $2N + 1$ carbon atoms. Although the binding energy of the polyene will include contributions from both the π network and σ bonds, the two parts can be handled independently by assuming σ-π separability and writing the energy as

$$V = \mathfrak{F}_\sigma + \mathcal{E}_\pi . \tag{1}$$

The localized nature of the σ electrons implies that the term $\mathfrak{F}_\sigma$ may be considered as a sum of contributions from individual C-C bonds:

$$\mathfrak{F}_\sigma = \sum_{i=1}^{N} f(r_i) . \tag{2}$$

The energy of the π electrons is calculated according to MO theory;

$$\mathcal{E}(N) = \pm [\beta_1^2 + \beta_2^2 + 2\beta_1\beta_2 \cos(2\pi j/2N + 1)]^{1/2} ,$$
$$j = 0, \pm 1, \pm 2, \cdots, \pm N, \tag{3}$$

where β_1 and β_2 (<0) are the transfer integrals between successive sites. In the absence of bond alternation $\beta_1 = \beta_2$, and the energy eigenvalues form a band of width $2Zt = 4|\beta|$. On the other hand, if one bond is longer than the other implying that $\beta_1 \neq \beta_2$, then a set of bonding and antibonding orbitals are formed in the ranges

$$\beta_1 + \beta_2 \leq \mathcal{E} < -\beta_1 + \beta_2 ,$$
$$\beta_1 - \beta_2 \leq \mathcal{E} \leq -\beta_1 - \beta_2 , \tag{4}$$

respectively. Since overlap integrals decrease exponentially in the separation distance, a reasonable assumption is that

$$\beta_1 = \beta_0 e^{-(a+x)/x_0}, \quad \beta_2 = \beta_0 e^{-(a-x)/x_0} , \tag{5}$$

where x is a small displacement of the atomic separation, x_0 is a typical radius of the $2p_z$ orbital, and β_0 is an energy (<0) with magnitude of the order of the π-electron ionization potential, and a is the uniform (undistorted) chain bond length. Using these expressions for $\beta(x)$ and Eq. (3), one obtains

$$\mathcal{E}_\pi = -2|\beta_a| \sum_{-N}^{0} \left(2\cosh\frac{2x}{x_0} + 2\cos j\theta \right)^{1/2} , \tag{6}$$

where $|\beta_a| = |\beta_0| e^{-a/x_0}$ is the transfer integral in the undistorted state and $\theta = 2\pi/(2N+1)$. The condition for equilibrium at $x = 0$ (i.e., *undistorted*) is

$$\left. \frac{\partial^2 V}{\partial x^2} \right|_{x=0} > 0 ,$$

or

$$\frac{\partial^2 \mathfrak{F}_\sigma}{\partial x^2} - \left(\frac{4|\beta_a|}{x_0^2} \right) \sum_{-N}^{0} \sec\frac{\pi j}{2N+1} > 0 . \tag{7}$$

The bond alternation instability is now obvious in that the first term is clearly proportional to the number of σ bonds ($2N + 1$), while the second term diverges like $N \ln N$ as $N \to \infty$. Hence, for an infinite polyene the stable configuration is one of unequal bond lengths. This result is no more than a restatement of the one-dimensional (1-D) Peierls instability[6,7] for a special case. For long polyenes where bond alternation becomes important the electron is subject to a periodic potential with a period of twice the original undistorted chain. Such a potential introduces a gap at $2k_F$ causing a change of character in the polyene from a metal to a semiconductor.

The importance of correlation in long chain polyenes has been stressed by Ovchinnikov *et al.*[8] and others.[9] Ovchinnikov *et al.*[8] argued that the electronic gap of ~2 eV seen in the long chain polyenes is due almost entirely to correlation with the Peierls effect playing little or no part. However, there is not general agreement on this point. Grant and Batra[10] estimated a somewhat larger single particle energy gap, whereas Duke *et al.*[11] showed that a calculation including a combination of bond alternation and Coulomb interaction yields results in agreement with photoemission and optical absorption data.

Linear polyacetylene, $(CH)_x$, is the simplest conjugated organic polymer (Fig. 1) and is therefore of special fundamental interest in the context of the above discussion. From theoretical and spectroscopic studies of short chain polyenes, the π-system transfer integral can be estimated as $|\beta_a| \simeq 2$-2.5 eV. Such an estimate implies that the overall bandwidth would be of order 8-10 eV; $W_\parallel = 2Z|\beta_a|$. However, the transverse bandwidth due to interchain coupling is much less. The nearest-neighbor interchain spacing[12] of 4.39 Å implies a transverse bandwidth ($W_\perp$) comparable to the bandwidth (longitudinal) in molecular crystals like tetrathiafulvalenium-tetracyano-p-quinodimethanide (TTF-TCNQ)[7]; thus $W_\perp \sim 0.1$ eV. Weak interchain coupling is therefore implied, and the system may be regarded as quasi-one-dimensional. Consequently, although the 1-D Peierls instability is not a full explanation of the electronic structure of polyacetylene, it provides a useful starting point of discussion for many of the electronic properties.

Interest in this semiconducting polymer has been stimulated by the successful demonstration of doping with associated control of electrical properties over a wide range[13,14]; the electrical conduc-

tivity of films of $(CH)_x$ can be varied over 12 orders of magnitude from that of an insulator ($\sigma \sim 10^{-9}\ \Omega^{-1}$ cm^{-1}) through semiconductor to a metal ($\sigma \gtrsim 10^3\ \Omega^{-1}$ cm^{-1}).[15-17] Various electron donating or accepting molecules can be used to yield n-type or p-type material, and compensation and junction formation have been demonstrated.[18] Optical-absorption studies indicate a direct band-gap semiconductor with a peak absorption coefficient of about 3×10^5 cm^{-1} at 1.9 eV.[19] Partial orientation of the polymer fibrils by stretch elongation of the $(CH)_x$ films results in anisotropic electrical[16] and optical[19] properties suggestive of a highly anisotropic band structure.[10] The electrical conductivity of partially oriented metallic $[CH(AsF_5)_{0.1}]_x$ is in excess of 2000 Ω^{-1} cm^{-1}.[16] The qualitative change in electrical and optical properties at dopant concentrations above a few percent have been interpreted[15,17,20,21] as a semiconductor-metal transition by analogy to that observed in studies of heavily doped silicon.

In this paper we present an experimental study of the lowest energy interband transition in polyacetylene and the free-carrier effects which result from heavy doping. Initial results on the optical properties were presented earlier in a brief communication.[19] The present work, a more detailed study including both absorption and reflection by films of cis- and $trans$-$(CH)_x$, is presented in an attempt to provide a more complete understanding of the electronic structure of this prototype semiconducting polymer. The experimental techniques are described in Sec. II. For pure $(CH)_x$, the experimental results are presented in Sec. III; the results for the heavily doped (with iodine or AsF_5) metallic polymers are given in Sec. IV. The absorption data for pure $(CH)_x$ are discussed in Sec. V in the context of the band structure and the role of Coulomb correlations in this quasi-1-D polymer. In Secs. VI and VII, we present a Kramers-Kronig analysis of the broad band reflectivity data to obtain the frequency-dependent conductivity and dielectric function, $\sigma_1(\omega)$ and $\epsilon_1(\omega)$, for the pure (semiconducting) and the heavily doped (metallic) polymers.

II. EXPERIMENTAL TECHNIQUES

Polyacetylene crystalline films were prepared using techniques similar to those developed by Shirakawa and Ikeda and collaborators[22] in the presence of a Zeigler catalyst with polymerization carried out at $-78\ °C$. Samples used in this study were either ~90% cis (as grown at $-78\ °C$) or 95% $trans$ (after thermal isomerization for 2 h at 200 °C).

Visible absorption measurements utilized thin films polymerized on the inner surface of a glass

reactor apparatus and were made on a Cary 14 spectrophotometer after inserting shielding material into the sample compartment to prevent scattered light from reaching the detector. The films were kept under vacuum during initial measurements; doping into the metallic range was carried out by subsequently introducing iodine or AsF_5 vapor. In order to calculate the absolute absorption coefficient it was necessary to obtain an accurate determination of the film thickness. These thickness measurements were performed after the completion of the optical measurements either by examination of calibrated electron micrographs or through use of an angstrometer. The measurement of a series of films resulted in thicknesses of about 0.1 μm; the resulting absorption coefficient was independent of the method used to determine the thickness.

Reflection measurements utilized free standing polymer films (thickness typically 0.05–0.1 mm). Orientation was achieved by stretching cis-$(CH)_x$ films at room temperature with subsequent additional stretching during isomerization at 200 °C. Details on the orientation techniques are presented elsewhere.[23] Reflectivity measurements in the middle ir through the visible utilized single beam spectrometers with the reflection from the sample compared to that of a mirror to obtain the absolute reflectance. All measurements were carried out at room temperature.

III. EXPERIMENTAL RESULTS: PURE $(CH)_x$

Absorption data for undoped $trans$-polyacetylene are presented in Fig. 2. The absorption coefficient begins a slow increase around 1.0 eV rising sharply at 1.4 eV to a peak at about 1.9 eV. The magnitude of the absorption coefficient (3×10^5 cm^{-1}) at the peak is comparable with the peak value in typical direct gap semiconductors of about 10^6 cm^{-1}.
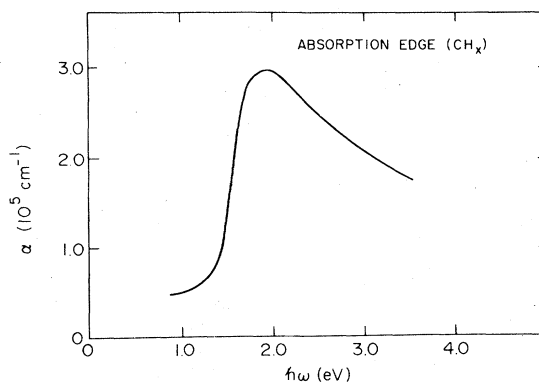
FIG. 2. Absorption coefficient as a function of frequency; $trans$-$(CH)_x$.

Similar absorption data for the *cis* isomer are presented in Fig. 3. Note that the absorption maximum is blue-shifted by about 0.3 eV–2.1 eV. There is also evidence of some structure around the peak absorption. The peak absorption coefficient ($\sim 4 \times 10^5$ cm^{-1} near 2.1 eV) is again comparable to that in typical direct-gap semiconductors.

Figure 4 shows the polarized reflectance data from oriented films ($l/l_0 \sim 2.5$–3) of pure *trans*-(CH)$_x$, where l_0 and l are the unstretched and stretched lengths, respectively. The earlier data[19] have been extended into the infrared down to 0.1 eV. The large optical anisotropy induced by orientation is clearly evident. The reflection data are consistent with a semiconductor model for pure (CH)$_x$ in qualitative agreement with the absorption data described above. The interband transition is apparent in $R_{\parallel}$ in the region of 2 eV with the reflectance decreasing to a low frequency value of $R_{\parallel} \simeq 0.1$, implying a dielectric constant of $\epsilon_{\parallel} \simeq 3$–4, in agreement with the value measured[20] at microwave frequencies [note that the low density of fibrils in the (CH)$_x$ films implies that the true value of $\epsilon_{\parallel}$ within a given fibril is $\epsilon_{\parallel} \sim 10$–12]. The perpendicular reflectance $R_{\perp}$ is small throughout the measured range indicative of quasi-one-dimensional behavior and relatively weak interchain coupling. The low frequency limiting value, $R_{\perp} \simeq 4\%$, implies $\epsilon_{\perp} \simeq 1.5$.

A quantitative comparison of the absorption and the reflectance spectra for *trans*-(CH)$_x$ is obtained by modeling the interband transition as a single Lorentz oscillator centered at 2 eV. Thus assuming

$$\epsilon(\omega) = 1 + \Omega_0^2/(\omega_g^2 - \omega^2 - i\omega\Gamma) \qquad (8)$$

leads to $E_g = \hbar\omega_g = 2$ eV, $\hbar\Omega_0 \simeq 4.0$ eV, and $\hbar\Gamma \simeq 0.54$ eV, the latter two parameters being determined by fitting to $\epsilon_{\parallel}(0)$ and $R_{\parallel}$ (2 eV). From these one estimates a peak absorption at 2 eV of $\cong 5 \times 10^5$ cm^{-1}
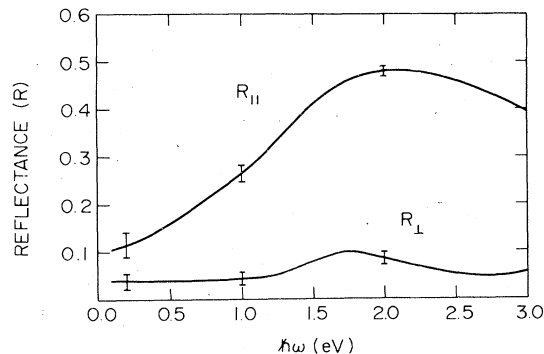
FIG. 4. Polarized reflectance as a function of frequency from partially oriented (CH)$_x$ ($l/l_0 = 2.5$). $R_{\parallel}$ and $R_{\perp}$ refer to light polarization parallel and perpendicular to the orientation direction.

in good agreement with Fig. 2. Note, that the implied quantitative agreement between the $R_{\parallel}$ data from partially aligned films and the absorption by nonaligned films implies that the strong absorption is polarized along the chain direction. We therefore conclude that the anisotropy is intrinsic and is present on a single fiber scale in the nonoriented polymer.

IV. EXPERIMENTAL RESULTS: DOPED METALLIC (CH)$_x$

The absorption data taken after various levels of iodine doping are presented in Figs. 5 and 6 for both isomers. After doping with iodine, the *trans* isomer shows a small decrease in the magnitude of the 2-eV transition, with additional absorption appearing at lower frequencies. The same general features are apparent in the iodine-doped *cis* polymer. Of particular interest is the observation of a significant change in the position and line shape

FIG. 3. Absorption coefficient as a function of frequency; *cis*-(CH)$_x$.
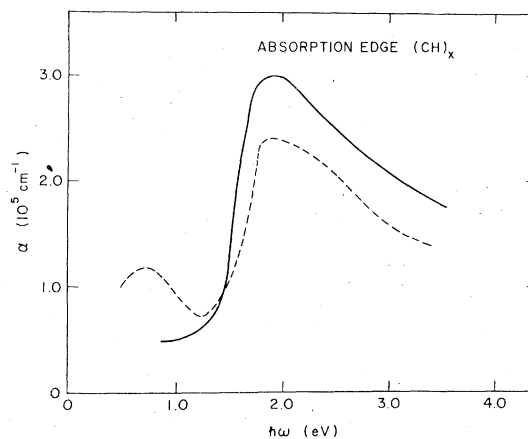
FIG. 5. Absorption coefficient as a function of frequency; *trans*-(CH)$_x$. Curve I reproduces the data of Fig. 2; curve II was obtained from the same film after doping with iodine.
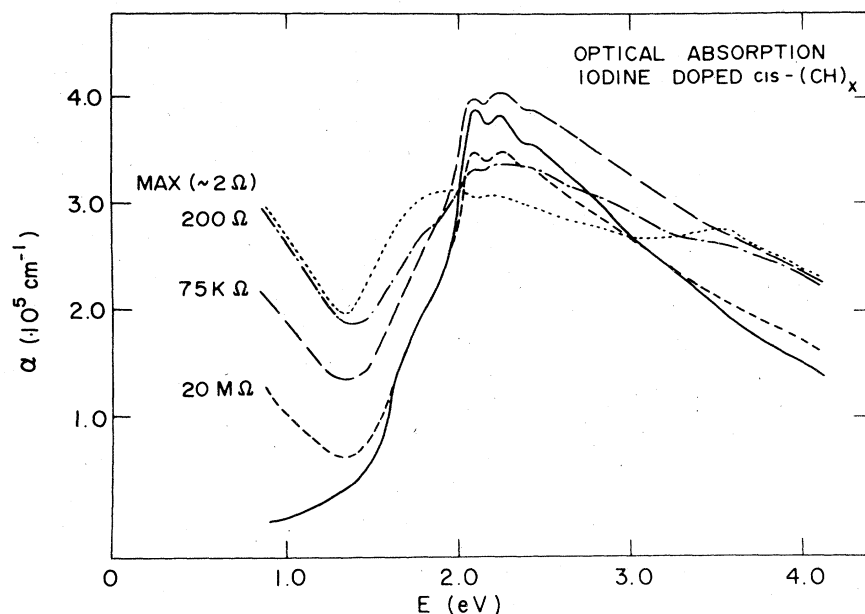
FIG. 6. Absorption coefficient as a function of frequency; cis-$(CH)_x$. The various curves represent various doping levels (iodine) as monitored by the film resistance; lowest resistance corresponds to the metallic limit. The solid curve is from undoped cis-$(CH)_x$.

after doping the cis polymer with iodine. The absorption spectrum of the cis isomer after doping is quite similar to that of the $trans$ isomer. This change suggests that isomerization occurs upon doping. Isomerization during doping is interesting in view of the fact that when the cis films are doped they regularly reach higher conductivity (by a factor of 2–5) than the (doped) $trans$ films. Because the $trans$ isomer is obtained from the cis by a thermally induced solid-state transformation, one might anticipate a larger number of defects in the

$trans$ isomer than in the cis starting material. Indeed, ESR studies[22,24] have shown approximately a tenfold increase in unpaired spins upon isomerization, consistent with localized defect formation. Cis-$trans$ conversion during doping and the higher conductivity with cis starting material would suggest that the resulting $trans$-$(CH)_x$ has fewer defects than that produced in the usual thermal isomerization.

In Fig. 7, absorption data for AsF_5-doped cis-polyacetylene are presented for several concentra-
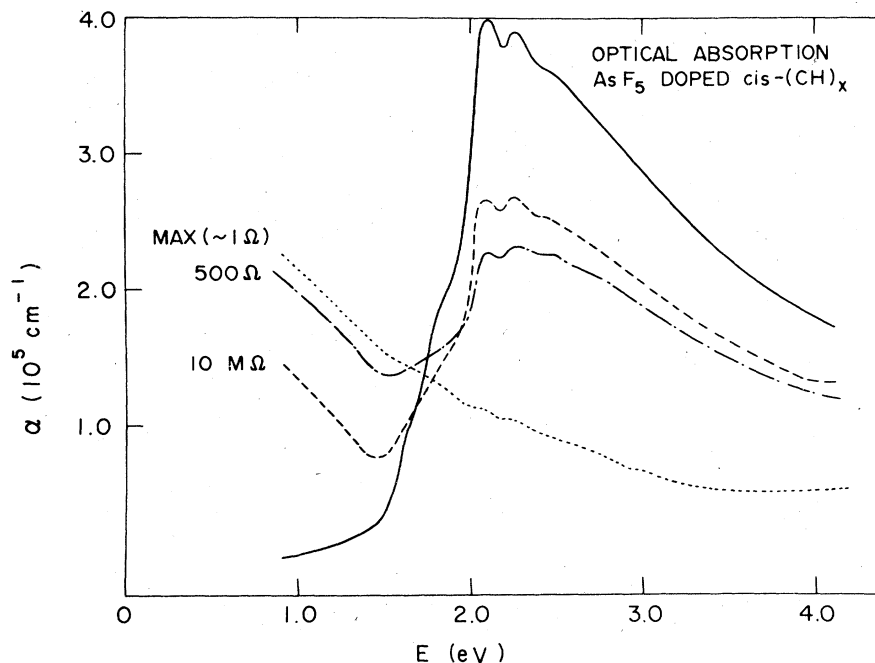
FIG. 7. Absorption coefficient as a function of frequency; cis-$(CH)_x$. The various curves represent various doping levels (AsF_5) as monitored by the film resistance. The solid curve is from undoped cis-$(CH)_x$.

tion levels of the AsF_5. The AsF_5-doped polymer does not show any change in line shape other than a decrease in intensity until the heaviest doping levels. At these high dopant levels the absorption is a simple monotonically decreasing function of energy, suggestive of free-carrier absorption. The absorption data of the AsF_5-doped polymer at the highest concentrations are quite different from the iodine data. The $\pi \rightarrow \pi^*$ absorption decreases significantly upon doping until only the slightest trace of the transition remains at the highest concentration.

Polarized reflectance data from oriented films of heavily doped metallic $(CH)_x$ are shown in Fig. 8 $[(CH(AsF_5)_{0.14})]_x$ and Fig. 9 $[(CH(I)_{0.20})]_x$. The parallel reflectance $R_\parallel$ is similar for the different dopants with two features of particular interest. First, the interband transition at 2 eV is clearly evident after doping, although reduced in intensity. Second, $R_\parallel$ increases in the infrared consistent with metallic behavior; at the lowest frequencies $R_\parallel$ approaches unity.

The absorption and reflection data for iodine-doped samples are consistent; both clearly show the interband transition at 2 eV and free-carrier metallic effects in the infrared. For the AsF_5-doped system the experimental situation is less clear. Examination of the reflectance data for metallic oriented films of $[CH(AsF_5)_y]_x$ shows the interband transition to be clearly evident, whereas at this high doping level the absorption data show little remaining of this transition. Moreover, as indicated above, the reflectance data from the AsF_5-doped polymer is quite similar to reflectance data from the iodine-doped polymer, Figs. 8 and 9. From this comparison and the overall similarity of properties of $(CH)_x$ films doped with either impurity, one would expect that the absorption
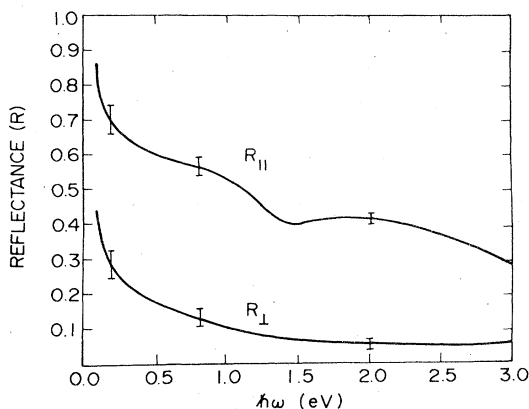
FIG. 8. Polarized reflectance as a function of frequency from partially oriented $(l/l_0 = 2.5)$ metallic $[CH(AsF_5)_{0.14}]_x$. $R_\parallel$ and $R_\perp$ refer to light polarization parallel and perpendicular to the orientation direction.
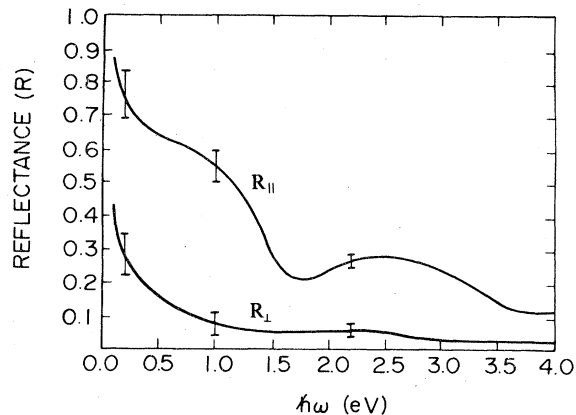
FIG. 9. Polarized reflectance as a function of frequency from partially oriented $(l/l_0 = 2.5)$ metallic $(CHI_{0.20})_x$. $R_\parallel$ and $R_\perp$ refer to light polarization parallel and perpendicular to the orientation direction.

data would be similar for either dopant, contrary to the results presented.

Experience with doping both isomers has provided some insight into the difficulties encountered in these comparisons. We have observed that in the case of AsF_5, if the films are doped too quickly or if unaligned films are used, then the result is the appearance of a golden color implying decreased reflectance in the blue part of the spectrum associated with the interband transition. Carefully doped *oriented trans-films* do not show such a color change. Since the absorption data were taken using unaligned films by necessity, the result was a golden appearance upon reflection. It is interesting to note that these absorption data on the AsF_5-doped polymer are quite consistent with the results of Grant,[10] who used unaligned doped films. Experiments are now in progress directed toward clarifying the source and nature of the uncertainties in the case of $[CH(AsF_5)_y]_x$. Primarily because of the consistent results obtained from reflectance and absorption studies in the case of iodine doping, we conclude that the π-π^* transition remains intact in the high-conductivity metallic regime. However, the optical properties in the metallic regime may be sensitive both to the dopant and to the precise doping concentration.

V. DISCUSSION OF ABSORPTION RESULTS FOR PURE $(CH)_x$

The transition rate for optical absorption from valence (v) to conduction (c) band is given by[25]

$$W_{cv} = \frac{e^2}{\epsilon_1 \pi m^2 \omega} \int d^3k \, |\hat{a}_0 \cdot \vec{p}_{cv}(\vec{k})|^2 \delta(\mathcal{E}_{cv}(k) - \hbar\omega) , \quad (9)$$

where the integral is over the Brillouin zone and $\mathcal{E}_{cv}(k) = \mathcal{E}_c(\vec{k}) - \mathcal{E}_v(k)$. Assuming that the main con-

tribution comes from one part of the zone and that the matrix element of the momentum operator $\vec{p}_{cv}(\vec{k})$ is slowly varying,

$$W_{cv} \simeq \frac{e^2 \langle \vec{p}_{cv}^2 \rangle}{\epsilon_1 \pi m^2 \omega} \int d^3k \, \delta(\mathcal{E}_{cv}(\vec{k}) - \hbar\omega) \qquad (10)$$

for one polarization of light.

This integral, often referred to as the joint density of states, simply counts the number of k values in the zone where the difference between the valence- and conduction-band energies is $\hbar\omega$. Because the values of $\vec{k}$ have a one to one correspondence in the valence and conduction bands, we only need consider the density of states in one band or the other. The integral can be written

$$\rho(\mathcal{E}_{cv}) = \int d^3k \, d^3k_0 \frac{\delta(\vec{k} - \vec{k}_0)}{|\nabla_k \mathcal{E}_{cv}(\vec{k})|_{\vec{k}=\vec{k}_0}} . \qquad (11)$$

In the typical three-dimensional case we can expand the energy surface as

$$\mathcal{E}_{cv}(k) = \mathcal{E}_0 + \beta_1 k_1^2 + \beta_2 k_2^2 + \beta_3 k_3^2 , \qquad (12)$$

leading to

$$\rho(\mathcal{E}_{cv}) = (\mathcal{E} - \mathcal{E}_g)^{1/2} / 4\pi^2 (\beta_1 \beta_2 \beta_3)^{1/2} . \qquad (13)$$

As anticipated, in a typical 3-D semiconductor the interband absorption turns on as the square root of the energy above the gap. However, as the transverse bandwidths tend to zero ($\beta_2, \beta_3 \to 0$) the density of states diverges. As the transverse bandwidth goes to zero we can treat the system as a one-dimensional semiconductor and write the dispersion relation for a one-dimensional tight binding band [see Eq. (3)]. In this case, the density of states near the gap edge varies as

$$\rho(\mathcal{E}) = N(0) / (1 - \mathcal{E}/\mathcal{E}_g)^{1/2} , \qquad (14)$$

where $N(0)$ denotes the density of states at the band center in the absence of an energy gap. Such a density of states would imply that the optical absorption instead of monotonically decreasing to zero rises toward the square root singularity indicated above.

For real solids the important question is how quickly the singularity is quenched for a small amount of transverse bandwidth. A semiquantitative demonstration of how the singularity is removed follows from

$$\rho(\mathcal{E}_{cv}) = \frac{1}{(2\pi)^3} \oint \oint \frac{dS}{|\nabla_{\vec{k}} \mathcal{E}_{cv}(\vec{k})|} , \qquad (15)$$

where the integral is over the constant energy surface. Provided that the energy is greater than $\mathcal{E}_g + W_\perp$, where $W_\perp$ is a transverse bandwidth, the constant energy surface will extend out to the zone boundary in the transverse directions. Thus the area becomes approximately $\oint \oint dS \simeq 2(2\pi/b)(2\pi/c)$,
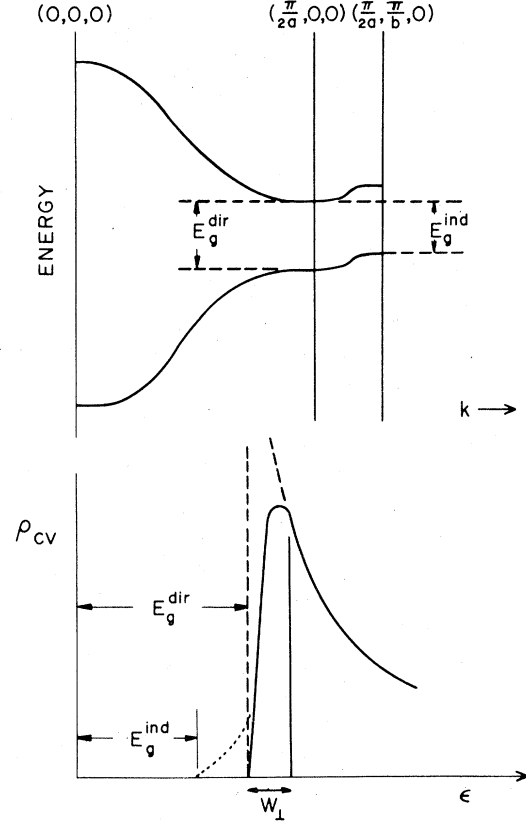
FIG. 10. (a) Schematic diagram of energy band structure of $(CH)_x$ showing the direct gap arising from the bond alternation. An indirect gap may result from interchain coupling, depending upon the precise interchain phase relation in crystalline $(CH)_x$. (b) The joint optical density of states corresponding to the band structure of Fig. 10(a). The rounding of the square-root singularity arises from interchain coupling ($W_\perp$).

where b and c are transverse lattice vectors. The gradient will be largely determined by $\partial \mathcal{E} / \partial k_\parallel$ but will include a small correction due to the transverse dispersion

$$|\nabla \mathcal{E}| \simeq [8\beta_1^2 a^2 (\mathcal{E}/\mathcal{E}_g - 1) + O(W_\perp^2)]^{1/2} . \qquad (16)$$

This result implies that $\rho(\mathcal{E}_{cv})$ will diverge as $N(0) / [(\mathcal{E}/\mathcal{E}_g - 1) + O(W_\perp^2)]^{1/2}$ until $\mathcal{E} \approx \mathcal{E}_g + W_\perp$. For $\mathcal{E} - \mathcal{E}_g < W_\perp$, $\rho(\mathcal{E}_{cv})$ decreases rapidly to zero at $\mathcal{E}_g$.

To illustrate these points we sketch the band structure of $(CH)_x$ in Fig. 10(a). The dispersion along the chain direction (a^*) assumes a π-bond transfer integral of $t_\parallel \simeq 2$ eV, while along the perpendicular direction Fig. 10(a) assumes $t_\perp \simeq 0.1$ eV consistent with the relatively large interchain separation. In the figure we have assumed positive dispersion on going from $(\pi/2a, 0, 0)$ to $(\pi/2a, \pi/b_\perp, 0)$. As a result there exists a direct gap at $(\pi/a, 0, 0)$ and an indirect gap from $(\pi/2a, \pi/b_\perp, 0)$

to $(\pi/2a, 0, 0)$. Consideration of a nearest-neighbor tight binding scheme shows that the detailed shape of $\epsilon(\pi/2a, k, 0)$ and $\epsilon_c(\pi/2a, k, 0)$ depends on the precise interchain phase relation in the crystalline $(CH)_x$.

The corresponding optical joint density of states is indicated in Fig. 10(b). The dashed curve represents the 1-D limit where the $(\mathcal{E} - \mathcal{E}_g)^{-1/2}$ singularity occurs at the band edge. Interchain coupling removes the singularity as described above shifting the maximum away from E_g^{direct} by an amount of order $W_\perp$. The possibility of an indirect gap is indicated by extending the curve below E_g^{direct}. Note, however, that indirect gap absorption requires phonon absorption or emission with a characteristic temperature dependence.

Collecting these results we can make a qualitative picture of the optical absorption for a highly anisotropic (quasi-1-D) semiconductor. The optical absorption will begin once the photon energy is larger than the indirect gap and then increase rapidly to the quenched singularity, decreasing for larger photon energies. Such a picture agrees with the data for polyacetylene shown in Fig. 2. Taking the absorption peak to be 1.9 eV, one estimates the transverse bandwidth to be ≤ 0.5 eV. This value for $W_\perp \sim 2zt_\perp$ is consistent with the intermolecular transfer integrals in other molecular crystals such as TTF-TCNQ. This interpretation of the optical absorption appears to be applicable to $(CH)_x$ as well as many other low-dimensional solids.

Using the above analysis as a guide one would estimate from the data a direct gap of ~ 1.4 eV. Experiments are planned to measure the onset of absorption as a function of temperature both to resolve the question of the existence of an indirect gap and to provide a better measure of the direct gap. The above discussion assumes the dominant energy dependence near the gap edge arises from the joint density of states. This should be a good approximation for the initial rise in $\alpha(\omega)$ below 2 eV since in the case where the energy gap is small compared to the overall bandwidth, the matrix element of the momentum operator is maximum at the gap edge and falls off as $(E_g/\hbar\omega)^2$ for $\hbar\omega > E_g$. The decrease in $\alpha(\omega)$ above 2 eV may in part arise from the energy dependence of $\langle p_{cv}^2 \rangle$.

Grant and Batra[10] have calculated the band structure by use of Hückel calculations and obtain an energy gap of 0.7–1.0 eV using various degrees of moderate bond alternation. These band calculations can be simply understood. In a tight binding calculation, the band gap due to bond alternation would be

$$\delta\beta = (\partial\beta/\partial x)_a \delta x = (\delta x/x_0)|\beta_a|,$$

where δx is the difference in bond lengths and x_0

and $|\beta_a|$ are defined in Eq. (5) and (6). If we assume δx takes the maximum value, equal to the difference in bond lengths between a single bond (1.51 Å as in ethane) and a double bond (1.34 Å as in ethylene), we estimate $\mathcal{E}_g \simeq 0.6$ eV. These simple ideas also provide an explanation of the 0.3-eV blue shift of the peak absorption in the *cis* isomer. The increased steric repulsion of the neighboring hydrogen bonds creates a slightly larger potential of the correct periodicity to increase the gap by the observed amount.

However, as indicated in the Introduction, this viewpoint is not universally accepted. Ovchinnikov *et al.*[8] have argued that the energy gap extrapolated to infinite-chain polyenes is too large to be accounted for by simple band theory of the dimerized chain, and they therefore concluded that Coulomb correlations play an important role. It has been shown[26] that the gap due simultaneously to correlation and a Peierls dimerization is of the form

$$\Delta \approx (\Delta_{corr}^2 + \Delta_{alt}^2)^{1/2}. \tag{17}$$

Various other theoretical studies have shown that Coulomb correlation may be important in this system. Duke *et al.* use a complete neglect of differential overlap, spectroscopically parametrized, version 2 (CNDO S2) calculation scheme on polyenes of varying lengths, $C_{4n+1}H_{4n+2}$ ($n = 1, 2, 3, 4$) to find an approximation to the band structure, electron photoemission spectra, and the lowest electronic transition energy. The ground state of the molecules is a totally symmetric Ag orbital. Using a configuration interaction analysis, Duke *et al.* also calculate the lowest B_u MO. The energy difference is then the lowest singlet molecular exciton. The exciton band is then extrapolated to $n \to \infty$ in order to predict the transition energy in polyacetylene, obtaining $\Delta E \simeq 2.0$ eV. The agreement between the extrapolated value and the experimental absorption edge is quite good.

It is clear that from this approach the $\pi-\pi^*$ interband energy is much larger than the calculated exciton energy (Duke *et al.*[11] estimate $E_{\pi^*} - E_\pi \simeq 5.5$ eV). The π^* energy calculated is the energy necessary to add one electron to the conduction band, and the π^* energy minus the π orbital energy is the photon energy necessary to excite an electron from the valence band to the conduction band. This simple analysis neglects correlation of the conduction electron and valence hole. In the traditional case correlation is added by using the effective-mass theory to estimate the electron-hole bound-state energy (exciton). Thus, as for the case of impurity centers in semiconductors, the problem can be reduced to a hydrogenlike solution, except that in the exciton case the center-of-mass frame does not correspond to the lattice

frame. The work of Duke $et\ al.$[11] would imply that this exciton binding energy below the conduction band is about 3.5 eV. Using a simple hydrogenic model, the 3.5-eV binding energy would imply a dielectric constant of $\epsilon_1 \sim 2$. This low value is in sharp disagreement with the value of $\epsilon_{||} \sim 10-12$ determined by microwave measurements at 10.6 GHz.[20] The measured value of $\epsilon_{||}$, on the other hand, leads to an estimate of about 0.1 eV for the exciton binding energy. However, this estimate rests upon the implicit assumption of weak correlations with the low frequency value of $\epsilon_{||}$ determined by the oscillator strength of the interband transition at ~1.4 eV. An equally valid interpretation of the experimental results can be constructed from the basis of a strongly correlated system. In this model the exciton binding energy is determined by $\epsilon_{||}(\omega)$ resulting from the $\pi \rightarrow \pi^*$ interband transition at $\simeq 5$ eV. The larger energy gap would imply a smaller dielectric constant $\epsilon \sim 2$ thus increasing the exciton binding energy to a magnitude consistent with the work of Duke $et\ al.$[11] The large low frequency dielectric constant would then be determined by the oscillator strength of the singlet exciton state at ~2 eV.

The data on absorption after doping is also important in the discussion. From Figs. 5 and 6 it is clear that the $\pi \rightarrow \pi^*$ transition remains visible in the iodine-doped film even up to the highest concentrations of iodine. The integrity of the $\pi \rightarrow \pi^*$ absorption is very important in considering the effects of excitons in the polymer since exciton lifetimes are extremely short in the presence of free carrier. This fact would imply that the iodine data exclude the possibility of the ex-

citon state in $(CH)_x$; however, the large binding energy clouds the issue. If we take the binding energy to be about 3.5 eV, using a dielectric constant of $\epsilon \sim 2$ the radius of the electron-hole pair can be estimated to be on the order of 1 Å. This distance is significantly smaller than the Fermi-Thomas screening length of free carriers even at the highest dopant concentrations. Thus on simple grounds one cannot assume that the exciton state should be completely damped out in the metallic regime of polyacetylene.

We summarize by stating that at this point all the optical data appear consistent with either of two models for the electronic structure of polyacetylene. The first view is simple single-particle (band theory) point of view, while the second view models $(CH)_x$ as a strongly correlated system where single-particle ideas are invalid. Since excitons may be viewed as bound electron-hole pairs, whereas a direct π-π^* transition would create a free electron and hole, direct observation of electron-hole pair generation through photoconductivity studies may provide a resolution of the problem. Early attempts[27] did indicate photoconductivity with onset below 1.5 eV consistent with a simple band point of view. We shall return to this point in Sec. VI through utilization of the oscillator strength sum rule.

VI. KRAMERS-KRONIG ANALYSIS: PURE $(CH)_x$

The Kramers-Kronig analysis[25] was used to analyze the reflectance data for partially oriented pure $trans$-$(CH)_x$. The results for $\sigma_1(\omega)$ and $\epsilon_1(\omega)$ are presented in Figs. 11 and 12. The results are
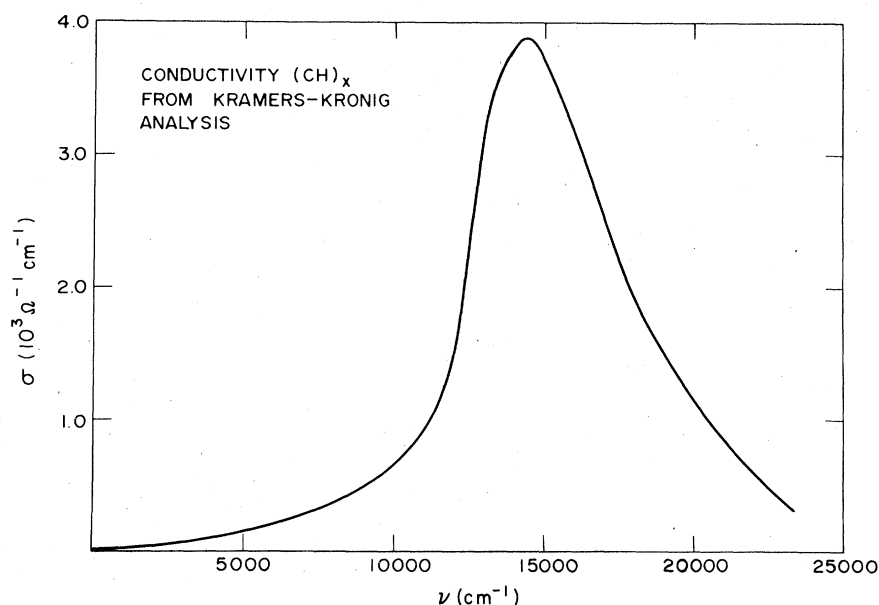
FIG. 11. $\sigma_{||}(\omega)$ for $trans$-$(CH)_x$ as obtained from Kramers-Kronig analysis of the $R_{||}$ reflection spectrum.

32.0

28.0

DIELECTRIC FUNCTION (CH)$_x$
FROM KRAMERS— KRONIG ANALYSIS

24.0

20.0

16.0

12.0

8.0

4.0

0.0

5000   10000   15000   20000   25000

-0.40

ν (cm^{-1})
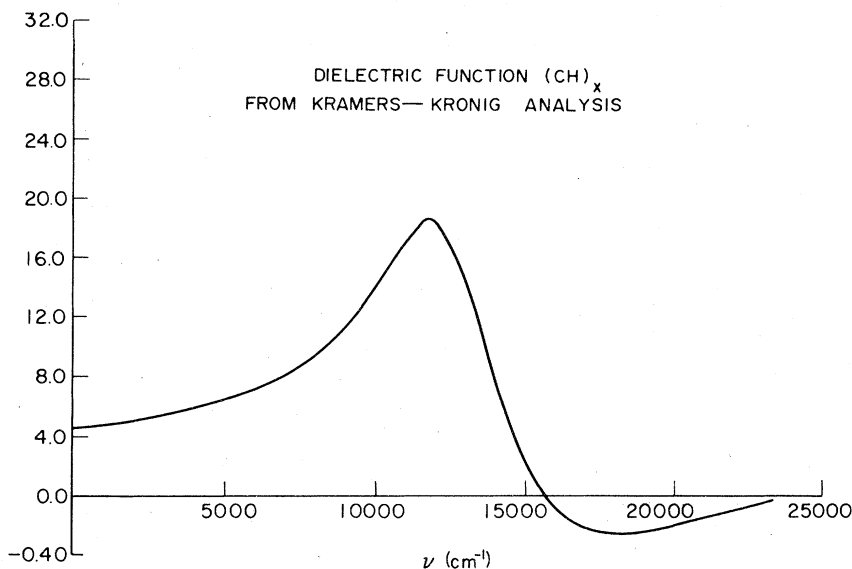
FIG. 12. $\epsilon_{||}(\omega)$ for *trans*-(CH)$_x$ as obtained from Kramers-Kronig analysis of the $R_{||}$ reflection spectrum.

precisely as expected for a semiconductor; $\sigma(\omega)$ rises from zero at low frequencies to a peak value of 4×10^3 Ω^{-1} cm^{-1} at about 16 000 cm^{-1}. The structure of $\sigma(\omega)$ is similar to that observed in other quasi-1-D semiconductors [see, for example, the results and discussion on TTF-TCNQ (Ref. 28) and K(TCNQ) (Ref. 29)]. $\epsilon_1(\omega)$ is negative at high frequencies crossing zero at about 16 000 cm^{-1}. At low frequencies ϵ_1 approaches a limiting value $\epsilon_1^{||}(0) \simeq 4$ consistent with the values determined directly from $R(\omega \to 0)$ and the microwave data.[20]

The oscillator strength sum rule can be used to obtain independent information on the optical effective mass, m^*;

$$8\int_0^\infty \sigma(\omega)d\omega = \omega_p^2 = (\omega_p^0)^2 \frac{m}{m^*}, \qquad (18)$$

where ω_p is the π-electron plasma frequency, $\omega_p^2 = 4\pi Ne^2/m^*$ and m is the free-electron mass. From the measured density[22] of (CH)$_x$ (0.4 g/ cm^3) we can estimate the number of π electrons per unit volume of the medium, $N \sim 2\times10^{22}$ cm^{-3}, implying $(\omega_p^0)^2 \sim 6\times10^{31}$. The experimental oscillator strength can be obtained by integrating Fig. 11; $8\int_0^\infty \sigma(\omega)d\omega \simeq (3\pm1)\times10^{31}$. The agreement is satisfactory. Moreover, we are certainly underestimating the experimental oscillator strength as a result of incomplete alignment of the polymer fibrils (x-ray[30] and electron microscopy[16] studies imply ~75% alignment). We conclude that nearly all the π-electron oscillator strength is contained in the 2-eV transition and that the effective mass is nearly unity, $1 < m^*/m < 1.5$. Note that the observation that the 2-eV transition exhausts the oscillator strength sum rule implies that it results

from the π-π^* interband transition rather than from an exciton transition, as discussed above.

From the values for $k(\omega)$ determined through the Kramers-Kronig analysis of $R(\omega)$, we can calculate the absorption coefficient $\alpha(\omega) = 2(\omega/c)k$. The calculated absorption coefficient is plotted in Fig. 13. Since the Kramers-Kronig analysis utilized polarized reflectance data from oriented films, the calculated $\alpha(\omega)$ is divided by 2 in Fig. 13 for direct comparison with the absorption data of Fig. 2. The good agreement indicates that $\sigma(\omega)$ and $\epsilon(\omega)$, as obtained from the Kramers-Kronig analysis of the reflectance, are accurate.

ABSORPTION (CH)$_x$

—— CALCULATED
--- OBSERVED

3.0

2.0

1.0

0

0   1.0   2.0   3.0   4.0

$\hbar\omega$ (eV)

α (10^5 cm^{-1})
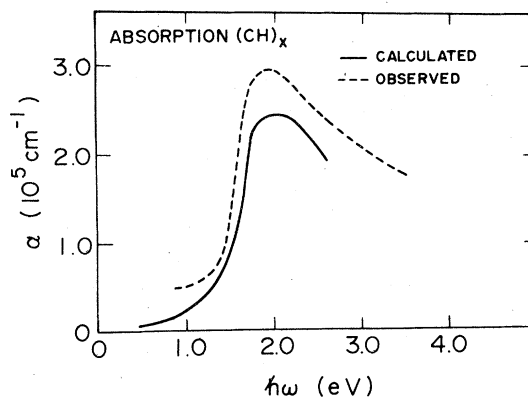
FIG. 13. Absorption coefficient of *trans*-(CH)$_x$ calculated using the optical constants obtained from Kramers-Kronig analysis of the $R_{||}$ reflection spectrum. The calculated $\alpha(\omega)$ was divided by 2 for direct comparison with the experimental absorption coefficient as obtained from nonoriented films.

VII. KRAMERS-KRONIG ANALYSIS: METALLIC $[CH(AsF_5)_{0.13}]_x$

A Kramers-Kronig transform has been used to analyze the reflectance data of metallic $[CH(AsF_5)_{0.13}]_x$. The data of Fig. 8 have been extrapolated to zero assuming a Hagen-Rubens behavior of the reflectance below 0.1 eV. Because the results of a Kramers-Kronig transform are very sensitive in the far infrared to the precise manner in which $R(\omega) \to 1$ as $\omega \to 0$, an accurate determination of $\sigma(\omega)$ in this frequency region is extremely difficult. However, we find that in the middle ir (above 1500 cm^{-1}) $\sigma(\omega)$ is insensitive to the details of the low frequency extrapolation. The results for $\sigma(\omega)$ are shown in Fig. 14. The broad peak in $\sigma(\omega)$ centered around 16 000 cm^{-1} results from the interband transition. The conductivity then begins to fall at lower frequencies until 11 000 cm^{-1}, where it again rises as one might expect for a system with free carriers. However, a somewhat surprising result is that below 6000 cm^{-1} the conductivity again decreases. This behavior is markedly different from the simple Drude behavior where $\sigma(\omega)$ is a monotonically decreasing function of frequency $[\sigma_{Drude} = \sigma_0/(1 + \omega^2 \tau^2)]$. The slow drop in $\sigma(\omega)$ continues until 1500 cm^{-1}, which is the lower limit of the present analysis. Between 1000 and 1500 cm^{-1} we find a weak dependence on the low frequency extrapolation with the behavior below 1000 cm^{-1} strongly dependent upon the extrapolation. Above 1500 cm^{-1} the results are independent of the extrapolation except for minor adjustments of the values in the third or fourth significant digit, details beyond the resolution of this analysis. The value $\sigma_{dc} \simeq 2 \times 10^3 \ \Omega^{-1} \text{cm}^{-1}$ found through direct dc measurements[16] on heavily doped (AsF$_5$) oriented samples of (CH)$_x$ is indicated in Fig. 14. Thus, the low frequency limit of this Kramers-Kronig analysis is quite consistent with other independent measurements. We conclude
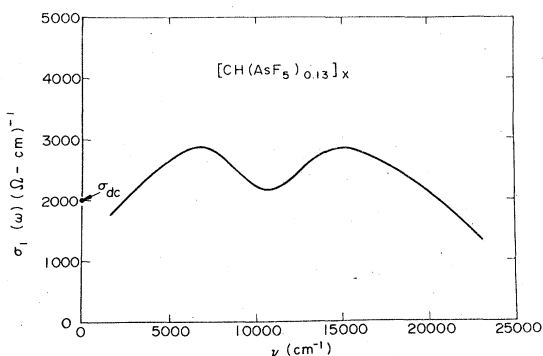
FIG. 14. $\sigma_{||}(\omega)$ for heavily doped metallic $[CH(AsF_5)_{0.13}]_x$ as obtained from the $R_{||}$ reflection spectrum.

that the decrease of σ below 6000 cm^{-1} is a real feature of $\sigma(\omega)$ and not an artifact of the extrapolation procedure.

Useful information can also be extracted by applying the sum rule relations to the data from the metallic state (Fig. 14). The effective number of electrons per molecule participating in the free-carrier optical transitions for energies less than the interband transition is given by

$$8 \int_0^{\omega_c} \sigma(\omega) d\omega = \frac{4\pi N e^2}{m^*} \eta_{\text{eff}}(\omega_c) , \qquad (19)$$

where $\eta_{\text{eff}}(\omega_c)$ is the fractional number of carriers contributing to the metallic conductivity. Using $\nu_c = 11\,000$ cm^{-1}, we find for the oscillator strength $8 \int_0^{\omega_c} \sigma(\omega) d\omega \simeq 4 \times 10^{31}$, i.e., approximately equal to the *total* π-electron oscillator strength in the polymer. The large oscillator strength therefore suggests that heavy doping removes the bond alternation leading to a uniform bond length polyene; a quasi-one-dimensional broad band metal with all π electrons contributing to the transport, i.e., $\eta_{\text{eff}} \simeq 1$. Such a picture is consistent with the small value of the density of states at E_F as inferred from magnetic susceptibility and thermopower studies.[21] On the other hand, after doping, Raman data continue to show the two carbon-carbon stretch frequencies (diminished in intensity),[30,31] and optical studies continue to show evidence of the unshifted interband transition (no Burstein shift), both characteristic of the bond alternated semiconductor. A possible explanation is an inhomogeneous metallic state (possibly resulting from inhomogeneous doping[32] within the fibrils) with undistorted metallic domains coexistent with regions of bond alternated semiconductor. Such a picture is consistent with all the data and explains the apparent absence of a Burstein shift upon doping, the residual Raman lines, and the observed sensitivity of the strength of the interband transition (after doping) to the different dopants.

The low frequency decrease in $\sigma(\omega)$ extrapolating toward the dc value cannot be understood in terms of a simple Drude-Lorentz model of the conductivity. However, it is intuitively clear that the fibril nature of the polymer will have a very strong effect on the dc transport properties. Moreover, if the metallic system is highly anisotropic on a microscopic scale as suggested by dc and optical studies of partially oriented films, impurities and defects will have an especially strong effect; in one dimension disorder leads to localization of states. Thus we anticipate that the low frequency transport will be limited by the imperfect polymer structure.

Electron microscopy photographs of (CH)$_x$ films show a fibril structure with typical fibril diame-

ter of about 200 Å.[16,22] The individual fibrils form a multiply coupled array through branching. Typical length to diameter ratio for the fibrils appear to be in the range of about 5–10. Therefore the polymer can be viewed as an effective medium made up of $(CH)_x$ fibrils at a volume filling factor of about $f = \frac{1}{3}$. For the as-grown films, the fibrils are randomly oriented in the plane; stretch orientation leads to partial alignment. From examination of the electron micrographs[16,22] and related x-ray data[30] we estimate approximately 75% alignment, i.e., the alignment factor, $\alpha \simeq 0.75$.

Within the doped $(CH)_x$ metallic fibrils the intrinsic frequency-dependent conductivity and dielectric functions are denoted $\sigma_1(\omega)$ and $\epsilon_1(\omega)$. The bulk properties of the metallic polymer can be related to $\sigma_1(\omega)$ and $\epsilon_1(\omega)$ through effective-medium theory. The problem of a composite medium was solved for isotropic spheres in an insulating matrix by Maxwell-Garnett[33] and has been recently discussed by Genzel and Martin,[34] by Barker,[35] and by Tanner, Sievers, and Buhrman.[36] The theory was extended to include anisotropy in shape and the conductivity and to include the effects of interacting particles by Tanner, Jacobsen, Garito, and Heeger.[28] Applying their results to the present case, we find the average medium conductivity

$$\langle \sigma_1(\omega) \rangle \simeq \frac{\alpha f \sigma_1(\omega)}{1 + [4\pi\sigma(\omega)/\omega]^2 g^2 (1 - \alpha f)^2}, \quad (20)$$

where f is the filling factor, α is the fractional alignment factor, and g is the typical depolarization factor $(g = (b/a)^2 [\ln(2a/b) - 1])$ for an ellipsoid of revolution, where b/a is the ratio of minor to major semiaxes. In writing the above expression, we have assumed that, consistent with the metallic behavior, $4\pi\sigma_1/\omega > |\epsilon_1|$. Moreover, as a result of the observed dc and optical anisotropy, we consider only the response to components of the applied field parallel to the $(CH)_x$ fibrils.

The important feature of Eq. (20) is that at low enough frequencies, the electric field within an "interrupted strand" is screened by the depolarization field due to the charge buildup at the boundary. The characteristic cutoff frequency ω_c is given by

$$[4\pi\sigma_1(\omega_c)/\omega_c] g(1 - \alpha f) = 1, \quad (21)$$

and corresponds to the condition when the depolarization factor in the denominator of Eq. (20) exceeds unity. From Fig. 14, we estimate $\omega_c \simeq 7000$ cm^{-1} at which point the (maximum) medium conductivity is approximately 3×10^3 Ω^{-1} cm^{-1}. Taking $\alpha f \simeq 0.25$ as described above, Eq. (20) yields $g \simeq 10^{-2}$, or $b/a \simeq 10^{-1}$, in good agreement with the fibril morphology. We therefore conclude from

the Kramers-Kronig analysis, that the fibril structure of $(CH)_x$ leads to metallic polymers which may be viewed as interrupted metallic strands.[37] The finite dc conductivity results from a combination of barrier penetration and phonon-assisted hopping[38] and will be considered in more detail in a subsequent publication. From the magnitude of the cutoff frequency we infer strand dimensions consistent with fibril dimensions observed in electron microscopy studies. Therefore the interrupted strands are tentatively identified with the branched fibrils; localization due to microscopic disorder appears to be relatively unimportant in these crystalline polymers.

We can obtain an estimate of the intrinsic conductivity within the individual metallic-doped $(CH)_x$ fibrils by inverting Eq. (20). At ω_c, the denominator is ~2, so that assuming $\alpha f \simeq \frac{1}{4}$, we find $\sigma_1(\omega_c) \simeq 2.4 \times 10^4$ Ω^{-1} cm^{-1}. The intrinsic dc conductivity is undoubtedly higher. If we assume a Drude dependence, $\sigma_1(\omega) = \sigma_0/(1 + \omega^2 \tau_0^2)$, where τ_0 is the Drude scattering time for the metallic state. It is difficult to obtain a direct measurement of τ_0 from the available data. However, the decrease in $\langle \sigma_1(\omega) \rangle$ observed from 7000 to 11 000 cm^{-1} in Fig. 14 implies that $\omega_c \tau_0 > 1$. Thus from this analysis we are able to estimate the intrinsic dc conductivity within a single fibril of metallic $(CH)_x$; $\sigma_{\text{intrinsic}}^{\text{dc}} \geq 2 \times 10^4$ Ω^{-1} cm^{-1}.

VII. SUMMARY AND CONCLUSIONS

In summary we have presented in this paper a detailed study of the optical and ir properties of semiconducting polyacetylene, $(CH)_x$, and the heavily doped metallic derivatives $(CHI_{0.22})_x$ and $[CH(AsF_5)_{0.13}]_x$. The reflection and absorption measurements when analyzed by means of the Kramers-Kronig relations provide detailed experimental information on $\sigma_1(\omega)$ and $\epsilon_1(\omega)$ for both the undoped semiconducting and the heavily doped metallic polymer.

The principal results for undoped semiconducting $(CH)_x$ are summarized as follows:

(a) Absorption data for *cis*-$(CH)_x$ and *trans*-$(CH)_x$ yield a peak absorption coefficient of approximately 3×10^5 cm^{-1} at 2.2 and 1.9 eV, respectively. Polarized reflectance data for the *trans*-isomer are qualitatively and quantitatively consistent with the absorption data.

(b) Kramers-Kronig analysis of the reflectance data for *trans*-$(CH)_x$ (polarized parallel to the fibril and chain orientation direction) yields $\sigma_1(\omega)$ and $\epsilon_1(\omega)$ typical of an interband transition in a semiconductor.

(c) Application of the oscillator strengths sum rule to $\sigma_1(\omega)$ for $(CH)_x$ indicates that nearly all the

π-electron oscillator strength is contained in the 2-eV transition and that the effective mass is near unity, $1 < m^*/m < 1.5$. The observation that the 2-eV transition exhausts the sum rule implies that it results from the π-π^* interband transition rather than from an exciton absorption.

(d) Analysis of the absorption data indicate a direct band gap of 1.4 eV and suggest an indirect gap at about 1.1 eV. From the shape of the absorption curve we estimate the transverse bandwidth $W_\perp < 0.5$ eV, consistent with a highly anisotropic band structure.

The principal results for heavily doped metallic $(CH)_x$ are summarized as follows:

(a) Transmission studies reveal the onset of free-carrier absorption in the infrared, consistent with metallic behavior.

(b) The π-π^* transition remains observable in the highly conducting metallic regime with no shift in frequency upon doping. However, the results appear to be sensitive to the dopant and to details of film preparation (e.g., as grown or partially oriented). For the iodine-doped polymer, absorption and polarized reflectance studies demonstrate that the π-π^* transition remains after doping. Similar results are obtained from reflectance studies of carefully doped oriented $(CH)_x$ after doping with AsF_5. However, transmission studies through thin films (nonoriented) of the AsF_5-doped polymer show only the slightest trace of this transition after doping. Inhomogeneous doping may be involved as indicated by x-ray photoemission studies.

(c) Absorption studies as a function of iodine concentration using cis-$(CH)_x$ starting material are consistent with cis-$trans$ conversion during doping, suggesting that the metallic polymer is the $trans$ form.

(d) Kramers-Kronig analysis of the polarized reflectance data yields $\sigma_1(\omega)$ and $\epsilon_1(\omega)$ consistent with interrupted strand behavior resulting from the interconnected fibril morphology of the $(CH)_x$ films. In particular, $\sigma_1(\omega)$ decreases in the infrared (below 6000 cm^{-1}) toward the dc value.

(e) Application of the oscillator strength sum rule to $\sigma_1(\omega)$ for the doped metallic polymer yields results which indicate that the total π-electron oscillator strength contributes to the free-carrier reflectance in the heavily doped polymer. This large oscillator strength suggests that heavy doping leads to an inhomogeneous metallic state with metallic domains coexistent with regions of bond alternated polymer.

(f) Analysis of the metallic $\sigma(\omega)$ with effective-medium theory implies an intrinsic dc conductivity for metallic $[CH(AsF_5)_{0.14}]_x$ of $\sigma > 2 \times 10^4$ $\Omega^{-1} cm^{-1}$. The measured dc values have thus far been limited by the low-density fibril morphology.

These optical studies have thus provided important information leading toward a more complete description of the electronic structure of long chain polyenes and a better understanding of the electrical transport in this emerging class of organic polymer conductors.

---

*Permanent Address: Asahi Chemical Industry, 2-1, Samejima, Fuji-shi 1416, Shiguoka-Ken, Japan.

†Permanent Address: Faculty of Science, Dept. of Chemistry, Nagoya University, Chikusa, Nagoya, 464, Japan.

[1] J. E. Lennard-Jones, Proc. R. Soc. A **158**, 280 (1937).

[2] C. A. Coulson, Proc. R. Soc. A **164**, 383 (1938).

[3] L. G. S. Brooker, J. Am. Chem. Soc. **73**, 1087, (1951); **73**, 5332 (1951); **73**, 5332 (1951).

[4] H. Kuhn, Helv. Chim. Acta **31**, 1441 (1948).

[5] H. C. Lounget-Higgins and L. Salem, Proc. R. Soc. A **25**, 172 (1959).

[6] R. E. Peierls, *Quantum Theory of Solids* (Oxford University, London, 1955), Chap. 5.

[7] *Low Dimensional Cooperative Phenomena*, edited by H. J. Keller (Plenum, New York, 1975); *Chemistry and Physics of One Dimensional Metals*, edited by H. J. Keller (Plenum, New York, 1977); *One Dimensional Conductors*, edited by J. Devreese (Plenum, New York, 1978).

[8] A. A. Ovchinnikov, I. I. Ukrainski, and G. V. Kventsel, Usp. Fiz. Nauk. **108**, 81 (1973) [Sov. Phys. Usp. **15**, 575 (1973)].

[9] A. Szabo, J. Langlet, and J. Malriev, Chem. Phys. **13**, 173 (1976); C. Cojan, G. P. Agrawal, and A. Flytzanis, Phys. Rev. B **15**, 909 (1977); M. Kertez, J. Koller, and A. Azman, J. Chem. Phys. **67**, 1180 (1977).

[10] P. Grant and I. P. Batra, Solid State Commun. **29**, 225 (1979); R. A. Harris and L. M. Falicov, J. Chem. Phys. **13**, 173 (1972); P. M. Grant, Bull. Am. Phys. Soc. **23**, 305 (1978).

[11] C. B. Duke, A. Paton, W. Salaneck, H. Thomas, E. W. Plummer, A. J. Heeger, and A. G. MacDiarmid, Chem. Phys. Lett. **59**, 146 (1978).

[12] S. Hsu, A. Signorelli, G. Pez, and R. Baughman, J. Chem. Phys. **68**, 5405 (1978); **69**, 106 (1978).

[13] H. Shirakawa, E. J. Louis, A. G. MacDiarmid, C. K. Chiang, and A. J. Heeger, Chem. Commun. 578 (1978).

[14]C. K. Chiang, M. A. Druy, S. C. Gau, A. J. Heeger, H. Shirakawa, E. J. Louis, A. G. MacDiarmid, and Y. W. Park, J. Am. Chem. Soc. 100, 1013 (1978).

[15]C. K. Chiang, C. R. Fincher, Jr., Y. W. Park, A. J. Heeger, H. Shirakawa, E. J. Louis, S. C. Gau, and A. G. MacDiarmid, Phys. Rev. Lett. 39, 1098 (1977).

[16]Y. W. Park, M. A. Druy, C. K. Chiang, A. J. Heeger, A. G. MacDiarmid, H. Shirakawa, and S. Ikeda, J. Polym. Sci. Polym. Lett. Ed. 17, 195 (1979).

[17]C. K. Chiang, Y. W. Park, A. J. Heeger, H. Shirakawa, E. J. Louis, and A. G. MacDiarmid, J. Chem. Phys. 69, 5098 (1978).

[18]C. K. Chiang, S. C. Gau, C. R. Fincher, Jr., Y. W. Park, A. G. MacDiarmid, and A. J. Heeger, Appl. Phys. Lett. 33, 181 (1978).

[19]C. R. Fincher, Jr., D. L. Peebles, A. J. Heeger, M. A. Druy, Y. Matsumura, and A. G. MacDiarmid, Solid State Commun. 27, 489 (1978).

[20]C. R. Fincher, Jr., M. Ozaki, A. J. Heeger, and A. G. MacDiarmid, Phys. Rev. B 19, 4140 (1979).

[21]Y. W. Park, A. Denenstein, C. K. Chiang, A. J. Heeger, and A. G. MacDiarmid, Solid State Commun. 29, 747 (1979).

[22]H. Shirakawa and S. Ikeda, Polym. J. 2, 231 (1971); H. Shirakawa, T. Ito, and S. Ikeda, Polym. J. 4, 460 (1973); T. Ito, H. Shirakawa, and S. Ikeda, J. Polym. Sci. Polym. Chem. Ed. 12, 11 (1974); T. Ito, H. Shirakawa, and S. Ikeda, J. Polym. Sci. Polym. Chem. Ed. 13, 1943 (1975); H. Shirakawa, T. Ito, and S. Ikeda, Die Macromoleculare Chemie 179, 1565 (1978).

[23]H. Shirakawa and S. Ikeda (unpublished).

[24]I. B. Goldberg, H. R. Crowe, P. R. Newman, A. J. Heeger, and A. G. MacDiarmid, J. Chem. Phys. 70, 1132 (1979).

[25]F. Wooten, *Optical Properties of Solids* (Academic, New York, 1972).

[26]Y. A. Bychkov, L. P. Gorkov, and I. E. Dzyaloshinskii, Sov. Phys. JETP 23, 489 (1966).

[27]A. Matsui and K. Nakamura, Jpn J. Appl. Phys. 6, 1468 (1967).

[28]D. B. Tanner, C. S. Jacobsen, A. F. Garito, and A. J. Heeger, Phys. Rev. B 13, 3381 (1976).

[29]D. B. Tanner, C. S. Jacobsen, A. A. Bright, and A. J. Heeger, Phys. Rev. B 16, 3283 (1977).

[30]H. Shirakawa (unpublished).

[31]G. B. Street (unpublished).

[32]W. R. Salaneck, H. R. Thomas, C. B. Duke, A Paton, E. W. Plummer, A. J. Heeger, and A. G. MacDiarmid, J. Chem. Phys. (to be published).

[33]J. C. Maxwell-Garnett, Philos. Trans. R. Soc. London 203, 385 (1904); 205, 237 (1906).

[34]L. Gensel and T. P. Martin, Phys. Status Solidi 51, 91 (1972).

[35]A. S. Barker, Jr., Phys. Rev. B 7, 2057 (1973).

[36]D. B. Tanner, A. J. Sievers, and R. A. Buhrman, Phys. Rev. B 11, 1330 (1975).

[37]M. J. Rice and J. Bernasconi, J. Phys. F 2, 905 (1972).

[38]P. Sheng, E. K. Sichel, and J. L. Gittleman, Phys. Rev. Lett. 40, 1197 (1978).